Frontiers in Nanotechnology

TYPE Review
PUBLISHED 25 October 2023
DOI 10.3389/fnano.2023.1257240

EDITED BY
Jan M. Macak,
University of Pardubice, Czechia

REVIEWED BY
Xingyun Li,
Qingdao University, China
Amit Kumar,
Pohang University of Science and Technology, Republic of Korea

*CORRESPONDENCE
Mariana Molina-Torres,
marian.mtt@hotmail.com
Ruben Mendoza-Cruz,
rmendoza@materiales.unam.mx

RECEIVED 12 July 2023
ACCEPTED 19 September 2023
PUBLISHED 25 October 2023

CITATION
Molina-Torres M, Hernández-Cristóbal O and Mendoza-Cruz R (2023), Small but mighty: unlocking the catalytic power of individual iridium atoms on titanium oxide.
Front. Nanotechnol. 5:1257240.
doi: 10.3389/fnano.2023.1257240

Small but mighty: unlocking the catalytic power of individual iridium atoms on titanium oxide

Mariana Molina-Torres[1]*, Orlando Hernández-Cristóbal[2] and Ruben Mendoza-Cruz[1]*

[1]Materials Research Institute, National Autonomous University of Mexico, Mexico City, Mexico, [2]National School of Higher Studies, Morelia Unit, National Autonomous University of Mexico, Morelia, Mexico

Single atom catalysts (SACs) have emerged as a rapidly developing field of catalysis research, with great potential for improving the efficiency and selectivity of many chemical reactions. SACs consist of isolated metal atoms dispersed on a support material, providing a unique and well-defined atomic structure and composition, allowing for precise control over their properties. In particular, iridium SACs are applied in numerous reactions, from electrocatalytic to photocatalytic applications. By the other hand, titanium oxide is a semiconductor with important applications as a reducible support for different catalyst, widely used in different reactions because of its high activity and stability. This review covers recent developments and frontiers in the particular system of Ir – TiO_2 SACs. It discusses the importance, synthesis, characterization techniques such as XPS, STEM, Differential Reflectance Infrared Fourier Transform, and XAS, and the applications of Ir – TiO_2 SACs. The review also explores the stability and durability of single-atom catalysts and the importance of understanding their structure-activity relationships to optimize their performance. A key dimension emphasized in this review is the importance of investigating the iridium-titania system. Iridium exhibits superior properties compared to other metals, particularly in maintaining stability as a single atom, owing to its resistance to sintering. Gaining a comprehensive understanding of and optimizing these factors are instrumental in unlocking the full potential of Ir – TiO_2 SACs. This route offers a promising trajectory towards enhancing catalytic performance across a spectrum of applications and facilitating the discovery of novel chemical reactions.

KEYWORDS

single atom catalysts, iridium, TiO_2, SACs, metal dispersed, active sites, characterization, electron microscopy

1 Introduction

Catalysis plays a central role in shaping our lives, over 90% of all chemical products have at least one catalytic step in their manufacture (de Vries and Jackson, 2012). Supported metal nanostructures are the most used form of heterogeneous catalyst in the industrial processes. Considerable endeavors have been dedicated to enhancing the effectiveness of supported metal catalysts downsizing the metal particles (Yang et al., 2013). The size of metal particle is a critical factor in determining the effectiveness of the catalysts, new findings from both theoretical and experimental studies have shown that clusters with sizes smaller than a nanometer exhibit enhanced catalytic activity and/or selectivity compared to particles of nanometer-scale dimensions (Herzing et al., 2008; Turner et al., 2008). There have been reports indicating that active sites often correspond to low coordination sites, such as unsaturated atoms

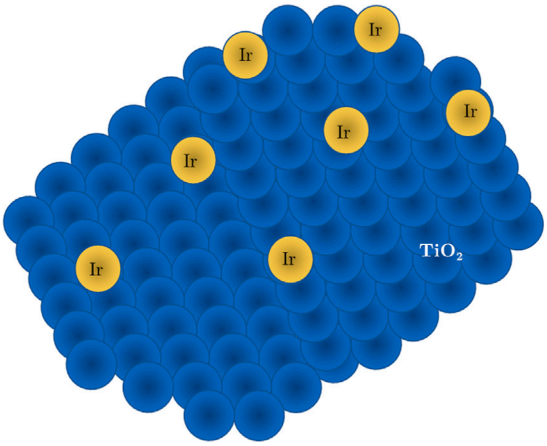

GRAPHICAL ABSTRACT
Ir catalyst supported by TiO_2.

(Remediakis et al., 2005). The size reduction also benefits the metal-support interactions, this phenomenon stems from the chemical bonding effect between the metal and the supports, as well as the associated interface, along with the charge transfer taking place between metal species and supports (Yang et al., 2013).

Late transition metals that are dispersed at the atomic level are often referred to as single atom catalysts (SACs). The SACs can be defined as a catalyst with isolated single atoms anchored onto its surface, capable of driving a catalytic reaction (Qiao et al., 2011). Generally, the single atoms are randomly and uncontrollably dispersed on the substrates. The interaction of these single-atoms with a metal oxide support can be different depending on its environment. The type of metal-support interactions regulates the electronic structure of catalysts, affecting the intrinsic activity of active sites (Samantaray et al., 2020). SACs can differentiate from other related single-site catalysts such as organometallic catalysts, in which in the latter case an organometallic complex are used to form the single-atom site, but keeping part of their ligands to achieve the catalytic reaction (Shan et al., 2022). SACs epitomize the utmost dispersion of a metal on a surface, with all the atoms being exposed. This holds paramount importance for the expensive and scarce noble metal catalysts, such as Ir, Pd, and Pt, which not only find the most applications but also attract significant interest for research purposes.

The significance of developing SACs becomes evident. Although the concept of having uniform active sites is highly appealing, the support structure in the vicinity of the single atom (SA) introduces heterogeneity to the active sites of the single atom catalyst (SAC, perhaps better conveys that the individual metal atoms are situated on the surface of another material) (Kottwitz et al., 2021). Consequently, the ideal uniform activity, which is characteristic of homogeneous catalysts, cannot be achieved. The combination of isolated single metals atoms with supports, gives rise to a distinct classification of catalysts. The synthesis of SAC presents a challenge, especially regarding the proper characterization of these materials, which is known to be inherently challenging owing to maximized atom utilization and precisely defining active centers, the direct observation of single atomic sites was not realized until the use of advanced characterization techniques such as atomic-resolution high-angle annular dark field scanning transmission electron microscopy (HAADF-STEM) which allowed imaging with atomic resolution (Li et al., 2019) that can directly measure the single atom to confirm the structure and conformation of the single metal atom, the chemical state of the metal center, and the conformation environment (Zonghua et al., 2020).

Supports play a critical role since they provide stability and enhance the efficiency of the catalysts. A common support is TiO_2 which has exhibited remarkable and intriguing properties. TiO_2 is a metal oxide with important applications in photocatalysis and oxidation reactions. Iridium, in turn, possesses excellent catalytic properties but its main limitation is its scarceness and high cost. Hence, iridium-based SAC improves the use of resources and, in combination with TiO_2 supports, represent excellent alternatives for the enhancement of catalytic activities towards different important reactions.

In this mini review, we centered in the recent developments and frontiers in the synthesis and characterization of SACs using TiO_2 as support, focusing on the stability and durability of SAC on TiO_2 and the importance of understanding their structure-activity relationships to optimize their performance. Despite the wide literature reviewing the field of SACs on different supports, this review gains importance in highlighting the contributions of TiO_2 supports forming SACs, in which much more limited information is available. First, a general view of the experimental finding about Ir as SACs is provided, reviewing its importance in catalytic reaction. Some common synthetic approaches to obtain SACs are summarized. Then, the experimental findings on $Ir - TiO_2$ SACs are introduced, discussing the common characterization techniques. Finally, applications and challenges of $Ir - TiO_2$ SACs and other metal oxide supports are reviewed.

2 Experimental findings about iridium as SACs

Fabrication of SACs is hard due to the tendency of single atoms to aggregate adds an additional layer of complexity, making it an even greater challenge. Elements with extremely low abundance on Earth are often the most active in catalytic reactions. This is precisely why optimizing the utilization efficiency of metal atoms and providing a greater number of exposed sites for reaction activation are crucial factors.

Iridium, the element with the 77th position on the periodic table, is classified among the 5 days transition metals. It crystallizes in a face-centered cubic (FCC) structure, but it stands as one of the most incompressible elements. Notably, iridium shares this distinction with other common metal centers that exhibit activity in numerous catalytic reactions. However, despite its potential, iridium has been limited in its exploration due to its scarcity in the Earth's crust and its high cost. As a result of their ability to undergo easy changes in oxidation state, iridium and its complexes find extensive use in catalysis for a wide range of industrial processes.

Single atom catalysts (SACs) offer a remarkable advantage in achieving 100% atomic utilization, serving as an exemplary strategy to significantly reduce noble-metal content without any compromise on catalytic efficiency. Hence, the study of metals, such as atomically dispersed iridium, does not impede the sustainable utilization of the metal. This exceptional property allows it to maintain its mechanical properties even at temperatures exceeding 2000°C and pressures up to 1.4 Mbar. Furthermore, iridium exhibits outstanding resistance to corrosion, making it highly suitable for a wide range of applications (Monteseguro et al., 2020).

TABLE 1 Summary of catalysts using iridium and different supports.

Single atom	Support	% Wt metal	Synthesis method	Application	Ref
Ir	ZIF-8	. . .	Impregnation Method	O.R.R.	Cao et al. (2019)
Ir	FeOx	0.01%	Co-Precipitation Method	Water-Gas Shift Reaction	Xiao et al. (2019)
Ir	MgAl2O4	0.20%	Wet-Impregnation	. . .	Bhirud et al. (2007)
Ir	ZrO2@C	0.60%	Pyrolysis	Hydrogenation of LA to GVL	Wang et al. (2022)
Ir	MgO	1%	Reported Method	Ethene Hydrogenation	Li et al. (2020)
Ir	TiO2 Rutile	1%	Impregnation Method	Catalytic Oxidation of ammonia	21
Ir	ZIF-8	1.20%	Pyrolysis	Formic Acid Oxidation	Shao et al. (2019a)
Ir	AP-POP	1.25%	Wet-Impregnation	Quasi-Homogeneous Hydrogenation Transformation of CO to Formate	Zhao et al. (2021)
Ir	H-Carbon ZIF-8	2.20%	Reported Method	O-H Carbenoid Insertion	Zhu et al. (2022a)
Ir	Co3O4	4.20%	Solid-State	Ammonia Production	Xiong et al. (2020)
Ir	C-N	4.40%	Pyrolysis	Epoxidation of Styrene	Shan et al. (2021)
Ir	Cobalt Oxide	4.93%	Surfactant-Mediated Method	O.E.R.	Wang et al. (2020)
Ir	NiO-CC	18%	Wet Immersion	O.E.R.	Xia et al. (2021)
Ir	N-C	40%	Pyrolysis	Electrochemical CO2 Reduction	Chen et al. (2018)

Noble metals of group VIII, such as Pd, Rh, Pt, and Ir, present outstanding catalytic activities, that together with transition metal oxide support catalyzes a wide number of reactions. In particular, iridium possesses a higher atomic mass compared to Pd and Rh, and it is the group with higher melting point. It possesses a versatile coordination chemistry, facilitating its dispersion in different metal oxide supports, such as MgO, FeOx, or $MgAl_2O_4$, with a strong interaction with the support (Lin et al., 2013; Pascarelli et al., 2019). For instance, Ir single-atom coordination with reduced Fe_2O_3, MgO, and TiO_2, corresponds to a substitutional configuration on the cation vacancies, with Ir coordinated with two oxygen atoms, which number could change after reaction (Xiao et al., 2019). A synergetic affect take place between the single atoms and their supports, lowering the reduction temperature of the support and generating a large amount of oxygen vacancies which contributes to their activity. The reducibility of the support also contributes to the stability of the single atoms, exhibiting high activity and selectivity.

Despite of this, few studies exist on Ir SACs in comparison with these other metals of the group, finding most applications in electrocatalysis. In this review, we aim to highlight the significance of studying this uncommon element when it is considered in its atomic form.

The pioneers in the field of catalysis utilizing iridium as an active center have posited that the success in fabricating single atom catalysts with iridium may be attributed to the remarkably low loading of the metal (Lu et al., 2019a). The probability of encountering short-range and long-range iridium-iridium interactions is estimated to be as minimal as 0.001 atoms nm^{-1}. Furthermore, upon increasing the iridium loading to 0.32%, a corresponding rise in observation frequency within the range of 0.5–1 nm was noted. Remarkably, no aggregation to sizes exceeding 1 nm was observed (Cao et al., 2019) therefore, it is advantageous to propose monodispersed iridium catalysts.

2.1 Summary of iridium as single atoms

In Table 1, examples of synthesis are presented where iridium has been used as a metal center on various supports, along with the synthesis routes employed and their applications.

Currently, there is ongoing research into synthesis methodologies aimed at creating Single Atom Catalysts, with wet impregnation being identified as the most promising approach. Although wet impregnation offers simplicity and scalability, it is important to acknowledge certain limitations. These include the challenge of achieving optimal metal loading and precise control over the anchoring position of isolated metal species on substrates, which can impact both catalytic efficiency and the feasibility of practical industrial applications.

2.2 Synthesis

The exploration and development of synthetic methodologies for single atom catalysts have become one of the most crucial research focuses. Fabricating single atom catalysts and maintaining the atomic dispersion of metal species under realistic synthesis and reaction conditions pose significant challenges. From a practical perspective,

TABLE 2 A comparison of different synthetic strategies, offering a comprehensive overview of their individual advantages and disadvantages.

Method	Advantages	Disadvantages	Ref
Wet chemical	Simple, low cost, easily scalable	Low metal loading, difficulty in managing metal atoms on substrates, strong dependence on synthesis factors	Haruta et al. (1987), Pham et al. (2023), Zanella et al. (2005)
Pyrolysis	Simple, large-scale production, inexpensive raw materials.	Uncontrollable metal sites on the selected substrates, instability of SA	Pham et al. (2023)
Electrochemical	Simple, controllable metal loading, relatively unexpensive	Uneven dispersion SA, limitation of thermodynamic control	Pham et al. (2023)
Photochemical reduction	Cost-effective, no extra treatment, controllable nucleation	sluggish nucleation growth rate, limited applicability	Pham et al. (2023)
Atomic Layer deposition	Controllable metal-loading, structure-performance exploration, Excellent uniformity and reproducibility. The loading of the SA could be adjusted through the number of cycles	High-cost equipment, slow synthetic process, high vacuum conditions, uncontrollable thickness and loading content, only materials with suitable ligands or functional groups could be chosen as support Not applicable for commercial preparation	Guo et al. (2022), Pham et al. (2023)
Atom trapping method	Simple, practical	High synthesis temperatures, requires a supply of mobile atoms and a support that can trap the mobile species	Guo et al. (2022)
Two-step doping method	Easy creation of vacancies on support and the high binding energies between the dopant and the vacancies, highly stable SACs	Limited to graphene	Guo et al. (2022)
Ball-milling method	Convert reactants into products during the reaction process, scale-up production, green	Not uniform sites, Requires high energy atom/ion generator,	Guo et al. (2022)
Photoreduction method	No special equipment, easy implementation	Catalytic active center not uniform	Guo et al. (2022)
In situ methods	Simple procedure, high dispersion, no metal loss	Limitation to specific systems, few references to a variety of metals	Liang et al. (2012), Cui et al. (2022)

an alternative and preferable approach is the development of wet-chemistry synthetic methods for single atom catalysts (SACs). This method offers easy operation and the potential for large-scale manufacturing. In wet-chemistry synthesis, mononuclear metal species are typically used as precursors. Therefore, implementing synthetic strategies to achieve atomically dispersed separation and isolation of the precursor, as well as preventing the migration and agglomeration of the formed single atoms, becomes crucial for successful SAC synthesis. These considerations are fundamental in ensuring the efficient and controlled production of SACs (Chen et al., 2018). Ir precursors are deposited onto the substrate surface using various wet-chemistry methods. This involves the metal precursors that are dispersed onto substrates through deposition-precipitation, coprecipitation, or wet-impregnation. Subsequently, reduction or activation procedures are carried out to form Ir-based catalysts with atomically dispersed Ir species. These steps are crucial in achieving the desired dispersion and isolation of individual Ir atoms on the substrate, enabling the synthesis of highly efficient catalysts with unique properties and reactivity (Pham et al., 2023).

2.2.1 Advantages and disadvantages of various synthetic approaches of SAC's

In Table 2, some advantages and disadvantages of various synthesis methods for obtaining SACs are presented (Pham et al., 2023).

The low metal content is mentioned as a disadvantage; however, for SACs, it is a notable advantage due to the reduced use of precious metals. Additionally, the possibility of industrial scalability is emphasized. Additionally, the potential for industrial-scale production is highlighted.

2.2.2 Deposition-precipitation with urea

Deposition-precipitation is a synthesis method commonly used in the preparation of catalysts. It involves the deposition of metal precursors onto a support material, followed by the precipitation of the metal species in the presence of a precipitating agent. This method allows for controlled and uniform distribution of the metal species on the support, resulting in catalysts with well-defined structures and properties. Deposition-precipitation offers advantages such as easy scalability, versatility, and the ability to tailor the catalyst composition by adjusting the deposition and precipitation conditions (Zanella et al., 2005; Qin et al., 2015).

The deposition-precipitation technique has been widely used to fabricate gold catalysts (Haruta et al., 1987; Haruta, 1997). In this method, the pH of an aqueous solution containing $HAuCl_4$ is carefully adjusted within the range of 6–10, taking into consideration the isoelectric points (IEP) of the metal oxide supports. This pH adjustment is crucial due to the amphoteric properties of $Au(OH)_3$, ensuring the formation of stable and well-dispersed gold species on the support material. The DP method offers ease of handling and provides control over the catalyst's composition and properties, making it a preferred choice in industrial catalyst production (Milone et al., 2010; Bokhimi et al., 2011; Qin et al., 2015).

2.2.3 Impregnation

The impregnation method is a technique used to deposit an active compound onto a porous surface or support. It involves immersing the support into a solution containing the active compound and allowing it to impregnate the porous surface through absorption. After impregnation, the support is subjected to drying or thermal treatment to remove the solvent and fix the active compound onto the support. This method offers great flexibility as it allows for control of the loading of the active compound and adjustment of the catalyst properties to specific application needs. It is widely employed in catalyst synthesis, particularly in the preparation of supported catalysts on porous solids (Van Dillen et al., 2003).

2.2.4 *In situ* techniques

Metal cations are chemically reduced to their metallic state by certain agents. In this state, they act directly as catalysts, facilitating chemical reactions involving the same agents. This process is straightforward and requires no additional purification. Consequently, it prevents potential catalyst loss or oxidation during the transfer process. By embracing this methodology, potential pitfalls associated with ligand presence, challenges stemming from uncontrollable variations in catalyst particle sizes, and concerns regarding mass loss or metal oxidation during purification and transfer procedures are all expertly sidestepped (Erdoğan et al., 2009; Liang et al., 2012; Cui et al., 2022; Zhang et al., 2022; Sun et al., 2023).

3 Experimental findings TiO_2 as support for Ir

Support materials play a crucial role in the stability and catalytic performance of single atom catalyst. These catalysts heavily rely on the support to provide a solid foundation for the deposition of active metal species. The choice of an appropriate support is of paramount importance as it directly influences the dispersion, accessibility, and reactivity of the active sites. Additionally, the support acts as a vital stabilizing agent, preventing the coalescence or aggregation of individual metal atoms and ensuring their sustained single-atom state during catalytic reactions. By offering a substantial surface area for the immobilization of metal atoms, the support facilitates efficient interactions with reactants, thereby enhancing catalytic reactions. Thus, meticulous selection and thoughtful design of suitable support materials are indispensable for the successful utilization of single atom catalysts in diverse catalytic applications.

Titanium is a metallic element that occupies the 22nd position in the periodic table. It is highly abundant in the Earth’s crust and exists in three main crystal forms: anatase, rutile, and brookite. Titanium is known for its exceptional strength-to-weight ratio, corrosion resistance, biocompatibility, affordability, and eco-friendliness (Ramos-Delgado et al., 2016). These properties make it a valuable material in various industries, as it offers a cost-effective and environmentally friendly solution. Titanium also serves a significant role in catalysis. TiO_2 are employed both as supports for catalysts and as catalysts themselves. These catalysts, including metal/TiO_2 and metal oxide/TiO_2 composites, play a significant role in diverse reactions such as hydrogenations, hydrodesulfurizations, selective oxidations, reductions, and Fischer-Tropsch processes. An additional notable feature lies in its capacity as a photocatalyst, which stems from its inherent semiconducting properties (Kominami et al., 1997; Scirè et al., 2021).

The proper selection of a catalyst support is crucial for enhancing the dispersion of active components and modulating the catalytic functionalities through metal-support interactions. The catalyst support significantly influences the overall performance and stability of the catalyst system, allowing for improved control over reaction rates and selectivity. It acts as a substrate that facilitates the anchoring and distribution of active species, providing a stable environment for catalytic reactions (Palcheva et al., 2013). The interaction between metal/TiO_2 has been studied as SMSI effect. The finding of heteroatomic metal-metal bonding suggested that titanium cations at surfaces might be capable of bonding to metal cations or metal atoms in a supported phase due to of the possibility of an interaction between the d orbital electrons of the surface cations and those of the supported metal atoms (Tauster et al., 1981).

As mentioned previously, other supports such as MgO, ZIF-8, and Al_2O_3 have been extensively explored in the literature for supporting iridium catalysts. However, titanium dioxide (TiO_2) has not been the preferred choice as a support material, which presents an area of opportunity for further investigation. TiO_2 offers distinct advantages, including its large surface area and high stability. Moreover, the use of the rutile phase of TiO_2 has been found to enhance the dispersion of the metal compared to other phases. The rutile phase provides a favorable environment for the dispersion of iridium species (Kim et al., 2018) promoting their accessibility and reactivity in catalytic reactions. This unique characteristic of the rutile phase, combined with the advantageous properties of TiO_2 as a support, makes it a promising candidate for supporting iridium catalysts. Exploring the potential of TiO_2, particularly its rutile phase, as a support material for iridium catalysts holds great promise in the development of highly efficient and selective catalytic systems.

4 Comprehending the nature of catalytic sites on the surface

X-ray photoelectron spectroscopy (XPS), transmission electron microscopy (TEM), including aberration-corrected high-angle annular dark-field scanning transmission electron microscopy (HAADF-STEM), diffuse reflectance infrared Fourier-transform spectroscopy (DRIFT), and X-ray absorption spectroscopies (XAS) are the key techniques employed for the analysis and authentication of iridium single atom catalysts (SACs). XPS allows for the investigation of surface composition and chemical states. HAADF-STEM provide atomic-scale resolution to directly examine the structure and coordination environments of isolated iridium atoms. DRIFT enables the study of molecular adsorption and surface species reactivity. With XAS it is possible to investigate a broad spectrum of surface structures. These techniques collectively play a pivotal role in the comprehensive characterization and understanding of iridium-based catalysts.

4.1 X-ray photoelectron spectroscopy

X-ray photoelectron spectroscopy (XPS) is a highly valuable technique employed in catalysis research for the analysis of catalyst surfaces. It serves the purpose of examining the surface composition and chemical states of catalyst materials. By utilizing X-ray photons to stimulate the ejection of inner-shell electrons from atoms within the catalyst, XPS enables the measurement of electron kinetic energy and intensity. This data provides crucial insights into the elemental composition, oxidation states, and bonding environments present on the catalyst surface (Greczynski and Hultman, 2020).

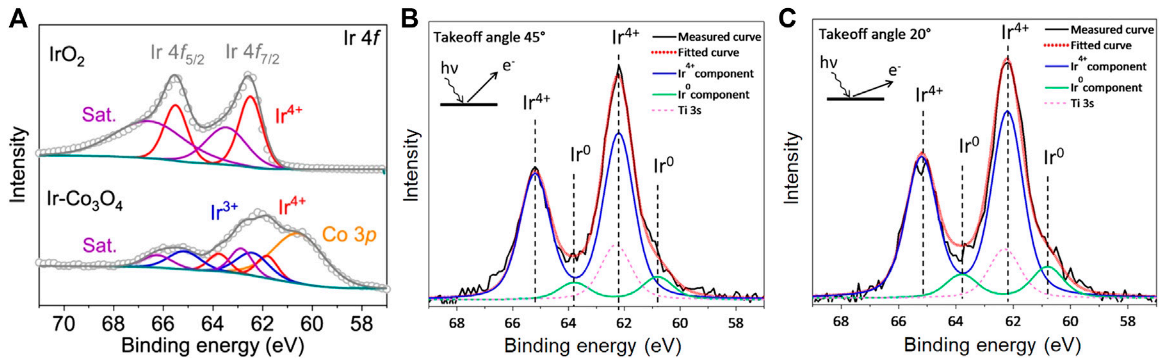

FIGURE 1
(A) XPS spectrum of characteristic Ir^{4+}. Adapted from Zhu et al. (2022b), licensed under CC BY 4.0. **(B,C)** Spectra of Ir^0, Ir^{4+}, and the overlap of Ti 3s. Adapted from Lee et al. (2018), licensed under CC BY 4.0.

In the realm of catalysis, XPS plays a pivotal role in elucidating surface chemistry and catalytic reactivity. It facilitates the investigation of active sites and their electronic structures, which are fundamental to catalytic processes. By employing XPS, researchers can explore changes in oxidation states of catalytic metals under reaction conditions, observe adsorbed species or reaction intermediates, and analyze the effects of environmental factors such as temperature and pressure on the catalyst surface (Oswald et al., 2013).

Moreover, XPS proves to be a valuable tool for pre- and post-reaction analysis of catalysts, allowing the detection of surface modifications, elucidation of catalyst deactivation mechanisms, and determination of catalyst stability. The technique can also be utilized for *in situ* characterization, enabling real-time monitoring of catalyst performance during catalytic reactions.

In summary, X-ray photoelectron spectroscopy is an indispensable technique in catalysis research, offering valuable insights into the surface chemistry and reactivity of catalysts. Its ability to probe the atomic-scale properties of catalyst surfaces provides crucial information for understanding catalytic mechanisms, optimizing catalyst design, and advancing the development of more efficient and selective catalytic processes. XPS enables the determination of the oxidation state of iridium, providing valuable insights into its chemical state.

In Figure 1A, Yiming Zhu et al. shows the XPS spectrum of IrO_2 displays a characteristic doublet at 62.5 and 65.4 eV, corresponding to the presence of Ir^{4+} species. On the other hand, for Ir-Co_3O_4, the Ir 4f spectrum exhibits two sets of doublets centered at 61.8/63.7 eV and 62.4/65.3 eV. These doublets can be attributed to the coexistence of Ir^{4+} and Ir^{3+} species, respectively.

In Figures 1B, C Lee et al. (2018) shows the spectra of the Ir $4f_{5/2}$ and $4f_{7/2}$ core level peaks are presented in Figures 1B, C. The deconvolution of the peak profile revealed the presence of both Ir^{4+} and Ir^0 components in the Ir:$SrTiO_3$ film. By measuring spectra at different takeoff angles, the depth distribution of the Ir^{4+} and Ir^0 components can be estimated due to the limited inelastic mean free path of photoelectrons in XPS measurements. Measurements performed at higher takeoff angles, which are more surface-sensitive, demonstrated a higher Ir^0 ratio (~13%) compared to measurements taken at a 45° angle (~10%). Interestingly, while tetravalent Ir^{4+} is expected based on DFT calculations for iridium atoms substituting Ti, the presence of metallic Ir^0 was observed.

X-ray photoelectron spectroscopy (XPS) analysis reveals the presence of metallic iridium supported on TiO_2, which holds significant importance as it signifies the catalytically active state of the material. The observation of metallic iridium on the surface of TiO_2 confirms its availability as an active species for catalytic reactions. Furthermore, the ability to deposit isolated iridium atoms at low metal loadings underscores the potential for achieving single-atom dispersion. This discovery unveils promising avenues for leveraging the distinctive reactivity and selectivity of single atom catalysts supported on TiO_2, thereby offering compelling prospects for catalytic applications.

4.2 Aberration-corrected scanning transmission electron microscopy

Transmission electron microscopy (TEM) is an advanced scientific instrument that employs a focused and accelerated beam of electrons to obtain detailed and high-resolution images of samples at the micro and nanoscale. By passing the electron beam through the sample, TEM can generate valuable information about the sample's internal structure, composition, and morphology. This technique relies on the interaction between the electrons and the atoms in the sample, producing signals that are captured by detectors and transformed into visual representations. With its exceptional resolving power, TEM enables researchers to explore the intricate details of materials, including the arrangement of atoms and the presence of defects or nanoscale features. There are two main transmission modes in TEM: the conventional TEM and the scanning transmission electron microscopy (STEM).

In conventional TEM, electrons coming from the electron source are focused on the sample in a wide and quasi-parallel beam, formed by the illumination system composed by electromagnetic condenser lenses, Figure 2A. These lenses are the responsible of forming the incoming beam and the manner of how it hits on the sample. Once the electron beam passes through the sample, the transmitted beam is collected by the objective lens and

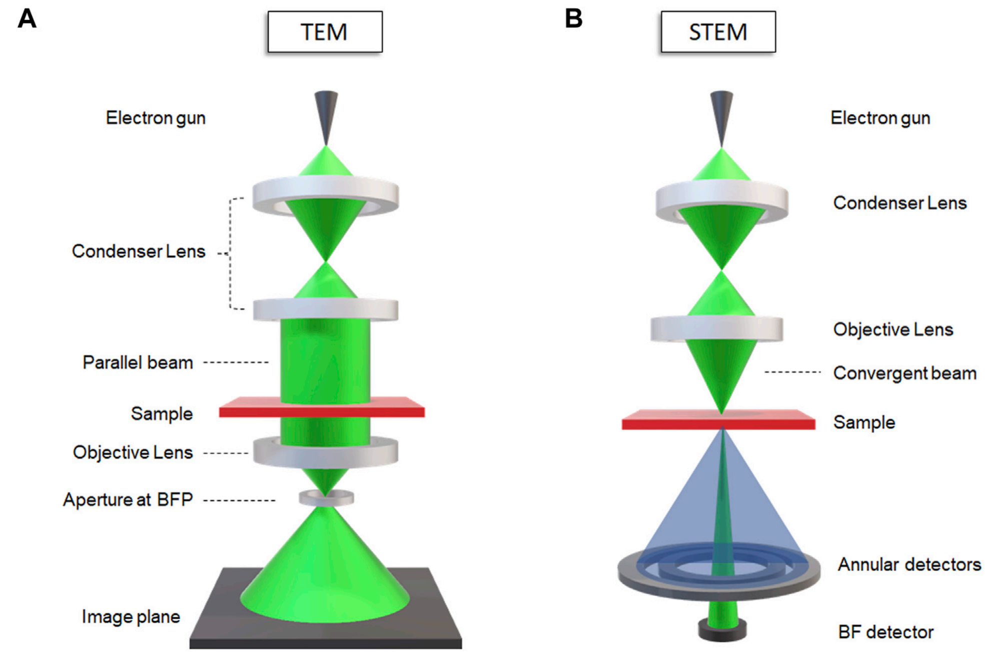

FIGURE 2
Sketch of the two main modes in TEM: conventional TEM **(A)** and STEM **(B)**.

projected to the screen. An image of the sample is instantaneously produced of all the illuminated area.

The incident electrons are described as a plane electron wave $\psi(r)$, which interacts with the sample and undergoes different dispersion phenomena. The exit electron wave at the end of the specimen plane, described as $\psi_{exit}(r)$, is formed by interference of the waves scattered by the atoms of the sample. These scattered waves are collected by the objective lens and focused at its back focal plane (BFP). If the lens is ideal and in focus, the recovered wave at the image plane, $\psi_{im}(r)$, should be:

$$\psi_{im}(r) = \psi_{exit}(r)$$

And the intensity distribution will be

$$I_{im}(r) = \psi_{im}(r)\cdot\psi^{*}_{im}(r) = 1$$

However, there is no perfect lenses, so the wave at the image plane will be:

$$\psi_{im}(r) = \psi_{exit}(r) \otimes OL(r)$$

where *OL(r)* is a function describing the behavior of the objective lens (Pennycook and Nellist, 2011; Deepak et al., 2015).

The phase shift produced by the lens can be described as (Carter, 2009):

$$\chi(u) = \pi\Delta f\,\lambda\,u^{2} + \frac{1}{2}\pi C_{s}\lambda^{3}u^{4}$$

Therefore, it is observed that the final image will depend on how the electron beam interacted with the sample and the phase shift produced by the objective lens, which in turn depends directly on the defocus *Δf*, the wavelength of the incoming electrons λ, and the spherical aberration constant, *Cs*. The interpretation of high-resolution TEM images is not straightforward because the image contrast will depend on our optical system, defocus conditions, sample thickness, and aberrations.

In STEM, instead of a wide and parallel beam, a highly focused convergent beam of electrons is scanned over the sample, Figure 2B. The electron probe is formed by the interference of an infinite number of plane waves at all the different convergence angles forming the illumination cone. No lenses are present below the sample, so the electrons that have interacted with the sample are collected directly by different detectors placed below the sample plane. The coherent beam is focused on each point of the sample, so the diffracted beams form discs that interfere to each other and provides the contrast interpreted as images, Figure 3A.

The amplitude of the waves is moderated by the partial coherence of the electron beam, which depend on the convergence angle and aperture size which limits the space from $-\mathbf{k}_{\max}$ to $\mathbf{k}_{\max}$ ($\mathbf{k}_{\max} = \lambda/\alpha$), Figure 3B. In real space, the amplitude of the electron probe $P(r)$ can be described as:

$$P(r) = \int A(k)\exp\left[i2\pi kr\right]dk$$

where $A(\mathbf{k})$ corresponds to a function of the circular aperture defining the convergence angle. In STEM, the upper objective lens is the one responsible of forming the electron probe, and will be affected by aberrations. The aberration coefficients have dimensions of length and can be expressed in power series of scattering angle θ as (Carter and Williams, 2016):

$$\gamma(\theta) = \frac{1}{2}\Delta f\theta^{2} + \frac{1}{4}C_{3}\theta^{4} + \frac{1}{6}C_{5}\theta^{6} + \frac{1}{8}C_{7}\theta^{8} + \cdots$$

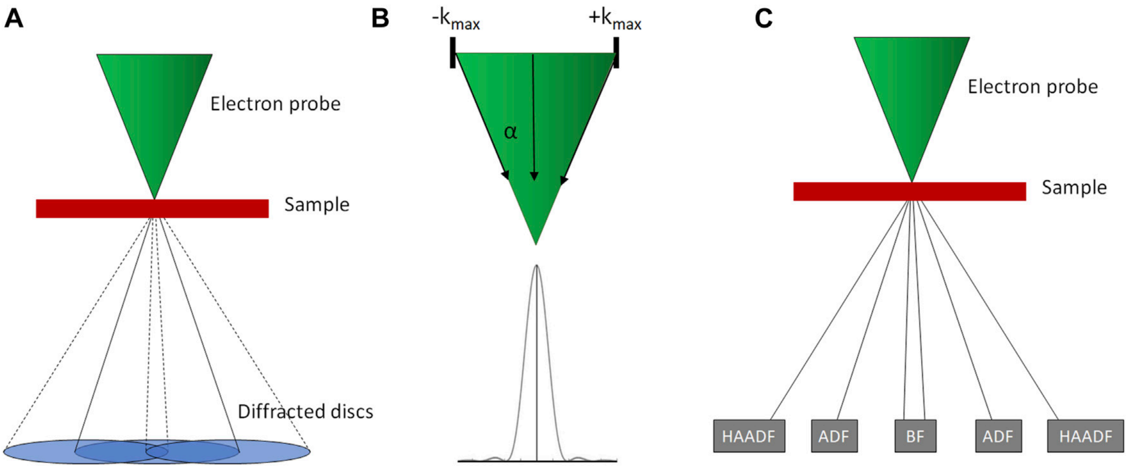

FIGURE 3
(A) The convergent electron probe form diffracted discs. **(B)** Schematics of the reciprocal and real space of the electron probe formed by coherent plane waves passing through an aperture defining a semi angle α. **(C)** Diffracted electrons from the sample are collected by detectors placed at different angles.

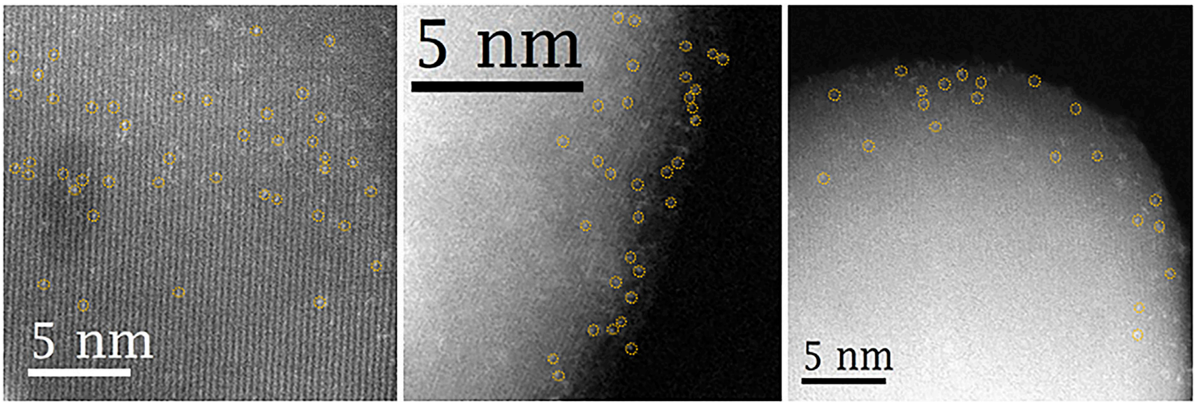

FIGURE 4
AC-HAADF-STEM measurements were employed to visually inspect the distribution of Ir in the 0.25% Ir/TiO_2 catalyst. Notably, no Ir nanoclusters were observed, and individual Ir atoms were identified as bright dots highlighted in yellow.

With $\chi = 2\pi\gamma$. The C_s coefficients are positive values. The amplitude of the STEM probe can be described as:

$$P(r) = \int A(k) \exp[i2\pi kr] \exp[-i\chi(k)]\, dk$$

And the probe intensity is its square $|P(r)|^2$.

In an uncorrected probe, the third order spherical aberration (C_3) can be compensated by negative defocus. In a spherical-aberration corrected probe, the next higher order aberration C_5 can be compensated by a slight negative C_3 (Carter and Williams, 2016). The optimal resolution for an uncorrected system can be expressed as:

$$d_{opt} = 0.43\lambda^{3/4}C_3^{1/4}$$

and for a *Cs* corrected system, the limiting resolution due to the *n*th order aberration:

$$d_{opt} = 0.45\lambda^{5/6}C_3^{1/6}$$

In a 200 keV aberration-corrected microscope, C_3 can be set to positive or negative values close to cero, while for an uncorrected high-resolution microscope C_3 is close to 0.5 mm. The electron probe diameter in STEM can be reduced through the aberration-corrected system, which consists of a hexapole-corrector with two multipole stages and it compensates all aberrations up to third order (CESCOR, 2023). Then, this small probe is scanned through the sample and interact with its atoms, which can be seen as an arrangement of individual scatters. Now the highly-convergent electron beam interacts individually with each scatter (instead of a wide parallel beam interacting with a large number of scatters in TEM). Each atom (a spike of potential) will scatter in proportion to the local probe intensity. Therefore, the intensity of the image can be written as:

$$I(r) = O(r) \otimes |P(r)|^2$$

i.e., the intensity at the image is the convolution of the object *O(r)* (array of scatters) and the probe intensity profile *P(r)*. The sharper the probe, the clearer the atoms are seen.

In STEM, when the beam is scanned over the sample, the collection of scattered electrons is done by the detectors placed below the sample, Figure 3C. The angle of scattering will depend on the atomic number Z of its constituent elements. Hence, detectors are placed to collect the scattered electrons at different angles, thus collecting different information of the sample. A bright-field detector (BF) collects those electrons scattered at low angles (~<10 mrad), and the images are similar to conventional TEM. An annular dark-field detector (ADF) can be placed to collect electrons scattered at higher angles (~10–50 mrad), which contain information of the chemical composition of the sample. A high-angle annular dark-field detector (HAADF) collects those electrons passing close to the atoms nucleus electrons, being scattered at much high angles (>50 mrad). These high-angle scattered electrons contain pure Z-contrast information from the sample and possess incoherent characteristics (Carter and Williams, 2016; Plascencia-Villa et al., 2020; Plascencia-Villa and Mendoza-Cruz, 2022).

STEM and TEM are powerful techniques widely used in catalysis research. One of the key features of these techniques is their ability to correct spherical aberration, allowing for high-resolution imaging at the atomic scale. With the advent of advanced electron microscopy instruments, aberration-corrected STEM offers the capability to visualize individual atoms and atomic structures in catalyst materials. This level of resolution is particularly valuable in the study of single atom catalysts (SACs), where the dispersion and arrangement of individual metal atoms play a critical role in their catalytic activity.

The aberration-corrected STEM/TEM imaging allows researchers to directly observe the presence and distribution of single atoms on the catalyst surface, and with the advantage of Z-contrast, atomic-resolution structural and chemical information can be obtained in a single image, Figure 4. This information is essential for understanding the relationship between atomic structure and catalytic properties, as well as for investigating the dynamics and behavior of single atoms during catalytic reactions.

Advanced AC-HAADF-STEM measurements were employed to visually inspect the distribution of Ir in the 0.25% Ir/TiO_2 catalyst. Notably, no Ir nanoclusters were observed, and individual Ir atoms were identified as bright dots highlighted in yellow. These Ir atoms were consistently located on the Ti sites of the TiO_2 support.

Individual Ir atoms were observed by AC-HAADF-STEM. The Ir sacs were resolved using an intensity profile since the observation was complicated due to the thickness of TiO_2 crystal. Nevertheless, it is possible to analyze the intensity profile and distinguish the presence of iridium atoms, Figure 5. These Ir atoms were consistently located on the Ti sites of the TiO_2 support.

4.3 IR/DRIFT

Diffuse Reflectance Infrared Fourier Transform Spectroscopy (DRIFTS) is a powerful analytical technique used in catalysis research for the characterization of catalysts and the investigation of surface species and adsorbed molecules. It utilizes infrared radiation to probe the vibrational modes of molecules on the catalyst surface. By measuring the changes in infrared absorption and reflection, DRIFTS provides valuable information about the surface chemistry, adsorption properties, and catalytic reactions occurring on the catalyst surface. This technique offers insights into the nature of active sites, the interaction between the catalyst and reactants, and the mechanism of catalytic reactions. It is a versatile tool for understanding the structure-function relationships of catalysts and designing more efficient catalytic systems.

DRIFTS works by irradiating the catalyst sample with infrared radiation and analyzing the resulting diffusely reflected light. The infrared radiation consists of a range of wavelengths that corresponds to the vibrational frequencies of chemical bonds in molecules. When the infrared light interacts with the catalyst surface, it is absorbed by the molecules present, causing them to vibrate and undergo changes in their dipole moment. These changes in dipole moment result in the scattering and reflection of the infrared light (Mitchell, 1993).

The diffusely reflected light is collected by a detector, such as a Fourier Transform Infrared (FT-IR) spectrometer, which measures the intensity of the reflected light as a function of wavelength. This spectrum provides information about the vibrational modes of the molecules on the catalyst surface, allowing for the identification of specific functional groups and the determination of surface species (Díaz et al., 2011).

By comparing the DRIFTS spectra of the catalyst before and after exposure to reactants or under different reaction conditions, researchers can gain insights into the adsorption and desorption processes, the formation of reaction intermediates, and the overall catalytic activity. The conducted studies have revealed the absorption band of iridium between 2075 and 2068 cm^{-1} (Díaz et al., 2011).

In Figure 6, the DRIFT spectra presented in this study demonstrate the adsorption of CO on catalysts that were reduced *in situ* in a hydrogen flow at 300°C. The iridium-based catalysts, namely, Ir/TiO_2 and Au-Ir/TiO_2-S, exhibited strong absorption bands in the range around 2100 cm^{-1}. These bands are characteristic of CO molecules adsorbed on iridium metal. The monometallic Ir catalyst showed a particularly intense absorption band centered at approximately 2068 cm^{-1}, accompanied by a broad contribution in the low-frequency side. These absorption bands in the region can be attributed to CO linearly adsorbed on various Ir^0 sites. Additionally, bands characterizing cationic iridium species were also observed in the spectral region between 2000 and 2107 cm^{-1} (Gómez-Cortés et al., 2009).

Rojas et al. (2015) showed that the Ir/TiO_2 catalyst exhibited a prominent absorption band with a pronounced peak at 2073 cm^{-1}, indicating the adsorption of CO on Ir^0 sites. Furthermore, it has been demonstrated that it is possible to deposit isolated atoms on TiO_2.

DRIFT is a valuable technique that plays a crucial role in the comprehensive characterization of the support surface. In the specific case of iridium catalysts supported on TiO_2, DRIFT analysis enables the direct observation of CO absorption bands, providing valuable insights into the presence and reactivity of iridium sites on the catalyst surface. The detection of CO absorption bands signifies that the iridium species maintain their reactivity and availability for catalytic reactions, despite the strong interaction and bonding with the TiO_2 support. This finding highlights the remarkable reactivity of iridium, which positions it as a highly promising catalyst for various catalytic applications. The ability to maintain its reactivity and accessibility on

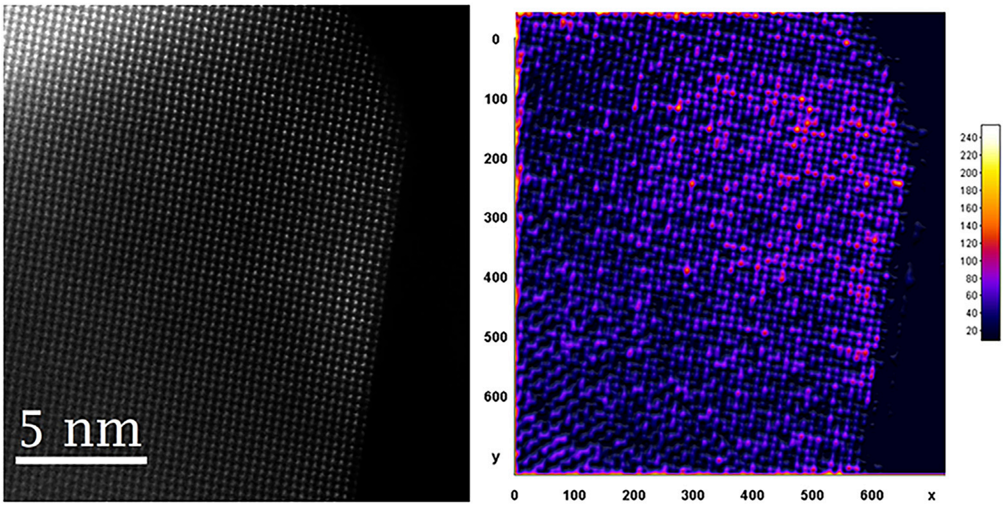

FIGURE 5
AC-HAADF-STEM of Ir in the 0.25% Ir/TiO$_2$ catalyst and its intensity profile.

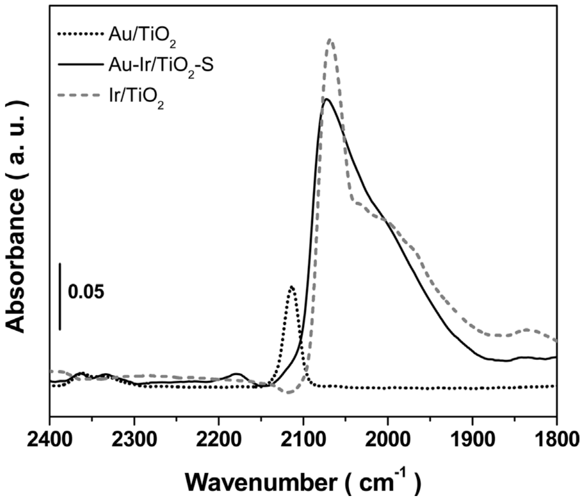

FIGURE 6
DRIFT spectra of Ir/TiO$_2$ 3.7 %wt (Adapted from Gómez-Cortés et al. (2009), with permission from Copyright © 2009 American Chemical Society).

the support surface makes iridium an attractive choice for catalytic transformations, offering opportunities for enhanced catalytic performance and selectivity in various chemical processes.

4.4 X-ray absorption spectroscopies

X-ray absorption spectroscopy (XAS) is currently being utilized to investigate a broad spectrum of surface structures. In the extended X-ray absorption fine structure (EXAFS) regime, single scattering is typically employed, enabling the straightforward determination of near-neighbor distances (R) and coordination numbers (A).

XANES is commonly affected by intra-molecular scattering, potentially providing straightforward insights into molecular orientation, intramolecular distances, and, consequently, the specifics of bonding with the surface. Moreover, it can reveal the atom's oxidation state, the chemical environment, and electronic transitions occurring near the central atom (Norman, 1986). XAS will only be shown in this review to observe the possibility of iridium binding in TiO$_2$.

EXAFS specializes in the examination of atomic arrangements around a central atom within a material, offering a meticulous investigation of its local atomic structure. This analytical method delves into the energy region situated beyond the critical point of X-ray absorption. EXAFS has a unique advantage over more standard methods like X-ray diffraction because one can directly determine the location of atoms surrounding each constituent separately (Sayers et al., 1970). In contrast, XANES concentrates on furnishing insights into the valency of atoms and their chemical environment, closely exploring the region proximate to the X-ray absorption edge. It is widely acknowledged that XANES exhibits sensitivity to the adsorption of various substances. Initially, we isolate changes in the metal's XANES data due to the presence of the adsorbate. This involves obtaining two separate XANES spectra: one for the metal with the adsorbate and another for the metal under different conditions, such as altered potential, current, or in a vacuum. The latter serves as the reference baseline. This technique can be viewed as a subtractive approach, aimed at isolating the influence of the adsorbate. Consequently, the resulting spectral shape provides insights into the chemistry, site symmetry, and quantity of adsorbed species on the surface (Ramaker and Koningsberger, 2010).

These two techniques synergistically complement each other and are jointly employed to achieve a comprehensive understanding of a material's structure and chemistry (Koningsberger and Prins, 1987).

X-radiation, when passing through matter, is absorbed through various mechanisms, including the photoelectric process, which involves the direct excitation of occupied core electrons to unoccupied levels see Figure 7 (Norman, 1986). The origins of EXAFS stem from fluctuations in the photoelectric cross-section

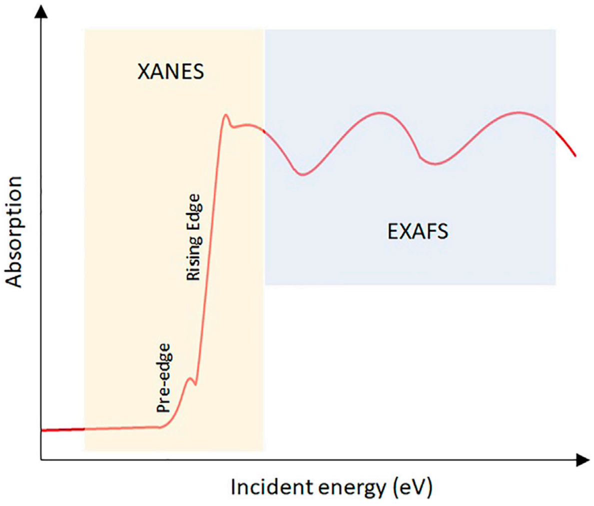

FIGURE 7
Schematic of the X-ray absorption spectrum, highlighting the different regions in which is divided.

resulting from the scattering of the emitted photoelectron by neighboring atoms encircling the absorbing atom (Sayers et al., 1971).

XANES is commonly affected by intra-molecular scattering, potentially providing straightforward insights into molecular orientation, intramolecular distances, and, consequently, the specifics of bonding with the surface. XANES directly examines the angular momentum of unoccupied electronic states, which can encompass bound or unbound, discrete or broad, atomic or molecular characteristics (Vaithianathan et al., 2006). Moreover, it can reveal the atom's oxidation state, the chemical environment, and electronic transitions occurring near the central atom (Norman, 1986). XAS will only be shown in this review to observe the possibility of iridium binding in TiO_2.

The chemical coordination environments of the Ir single atom species were investigated by acquiring extended X-ray absorption fine structure (EXAFS) data at the L_3-edge of the Ir species, using the Ir/AC nano catalyst for comparison with other standard Ir compounds.

Porous organic polymers based on aminopyridine show that Ir's closest neighbors are Ir-Ir and Ir-O. This result can explain the presence of Ir metal on the surface. The fitted EXAFS data indicate the presence of Ir-Cl, suggesting that the Ir species existed as isolated metal atoms and possibly maintained their high coordination number as a result of ligand exchange with the support. In summary, EXAFS data show that mononuclear Ir is situated on the framework using $-Cl_2$, $-O_2$, or -OH groups as ligands. The Ir single atom species was evidently coordinated by two neighboring oxygen nuclei associated with the support (Shao et al., 2019b).

In atomically-dispersed iridium on tin oxide, they performed *ex situ* and *in situ* X-ray absorption spectroscopy and have shown data in R-space that correspond to Ir-O, with a lack of strong contributions from Ir-Ir or Ir-O-Ir interactions. They conducted this study to investigate the oxygen evolution reaction (OER) mechanism, for which they computed the mechanisms using the structures of $Ir\text{-}_{SAC}$-ITO. In these structures, they've demonstrated the binding of Ir sites with oxygen. In this study, they observed IrO_2 (Ir_{IV}). The oxidation states of Ir were assigned as Ir_{III}, Ir_{IV}, and Ir_V (Lebedev et al., 2020).

In Figure 8, the researchers constructed computational models based on Ir-SAC, and these models illustrated the coordination of Ir atoms with oxygen sites present on the support material. Within the proposed mechanism, the researchers further elucidated the bonding interactions by showcasing how the Ir sites form bonds with hydroxyl (OH) groups. This detailed analysis provides valuable insights into the intricate chemical processes occurring at the atomic level, shedding light on the catalytic behavior of $Ir\text{-}_{SAC}$ in various reactions, including the oxygen evolution reaction. Computed studies of iridium nanoparticles using density functional theory calculations have shown that the planar configurations are more stable than the three-dimensional ones, with each arranged in decreasing order of stability (Pawluk et al., 2005).

In the analysis of Ir/TiO_2 for CO oxidation, both EXAFS and XANES techniques were used to understand the rate-controlling steps for CO oxidation. Ir single-atom sites within the catalyst were found to be uniformly distributed.

DRIFT spectrum of the Ir_1/TiO_2 catalyst in Figure Xb shows two CO bands at 2077 and 1995 cm^{-1}, attributed to Ir gem-dicarbonyl ($Ir(CO)_{2\text{-support}}$).

In Figure 9 (Xanes region), the EXAFS spectra reveal a dicarbonyl state (two Ir-CO). Besides, the model fit indicates two Ir-O bonds from the support and one Ir-Ti bond. XAS results indicate Ir initially exists as $Ir(CO_2(O)_2$ after reduction and gets oxidized to $Ir(CO)\ (O)_3$ during/after reaction. For the Density Functional Theory (DFT) calculations (Figure 9), we opted for adsorbed Ir single atoms to represent the experimental structure. This choice was made because these Ir single atoms can potentially form a dicarbonyl in the CO-reducing environment. It is important to note that Ir single atoms embedded within the TiO_2 lattice could not maintain a stable dicarbonyl structure.

It is imperative to underscore that this investigation was undertaken using TiO_2 in the anatase phase. Consequently, it is strongly advised to contemplate a parallel inquiry employing rutile TiO_2, as the variations in the crystalline phase can yield distinctive outcomes.

5 Exploring the catalytic capabilities of iridium: applications

$Ir\text{-}_{SACs}$ have been applied widely in numerous applications, in particular, in electrocatalytic reactions, such as ORR, water splitting, CO_2 reduction, HER, epoxidation of ethylene (Yang et al., 2023). Ir on TiO_2 as a SAC, is a more specific system that has been applied in oxidation and reduction reactions, photocatalysis, electrocatalysis. Here, we review some application of Ir SACs supported on metal oxides.

5.1 Oxidation reactions

Carbon monoxide (CO) and ammonia oxidation are important reactions, since they are harmful residual gases from the incomplete combustion of industrial compounds. By the other hand, CO oxidation is a model reaction for the fundamental understanding

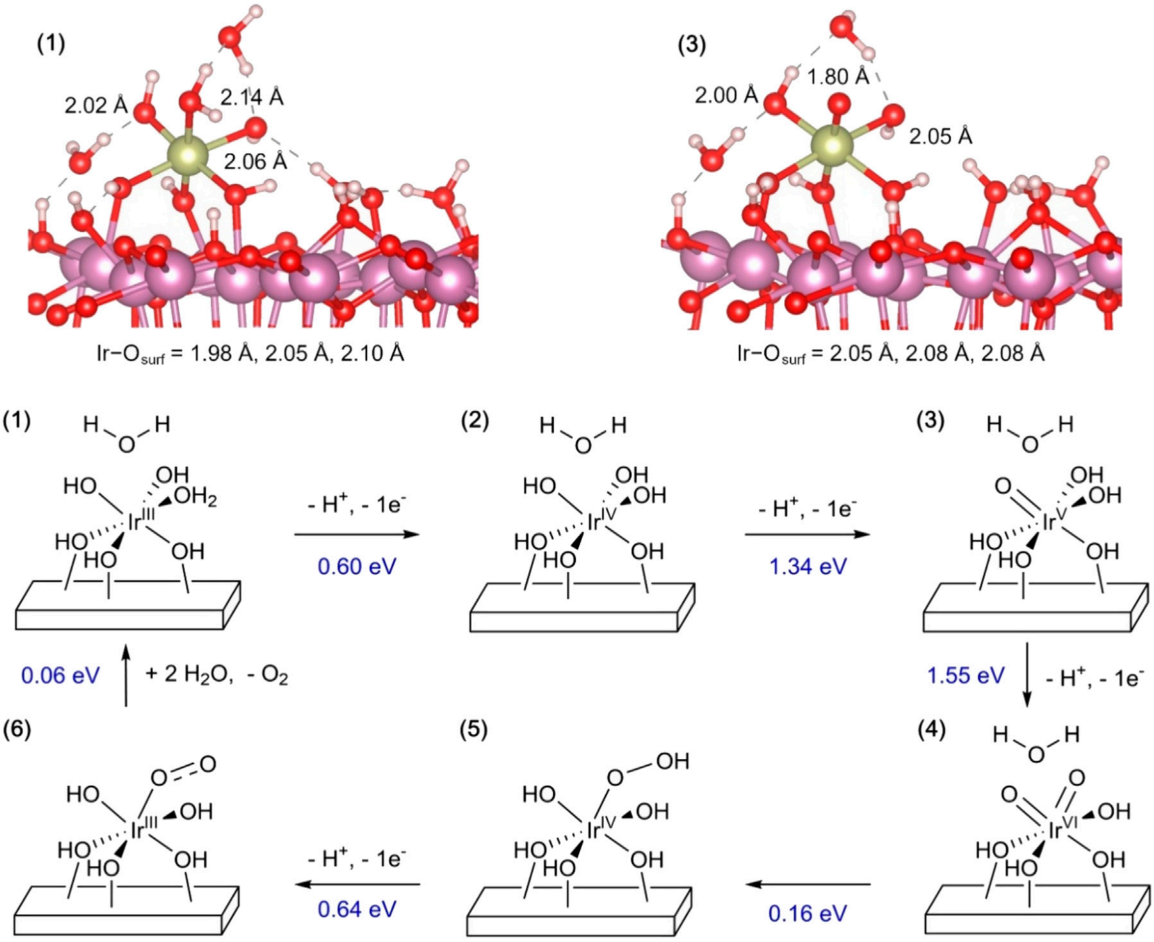

FIGURE 8
Computed OER with the structures of Ir-$_{SAC}$-ITO. Reproduced from Lebedev et al. (2020), with permission from Copyright © 2023 American Chemical Society, licensed under CC BY 4.0.

of catalytic processes which can be applied to generate products of industrial relevance. Hence, efforts to improve this reaction in which Ir-based SACs play an important role have been done.

Jian Lin and coworkers designing an Ir-Fe(OH)x catalyst which stabilized Ir single atoms for the oxidation of CO. HAADF imaging showed that Ir single atoms distributed uniformly over the support, with small clusters below 1 nm. The adsorption and activation of O_2 was promoted by the support, reflecting its erole in the activity of Ir-based catalysts for the CO oxidation (Lin et al., 2012). Lu Dai and collaborators, reported the promotion of CO oxidation of Ir-TiO_2 catalysts. The promotion was achieved by the tuning of the metal-support interaction, induced by the incorporation of small amounts of CeO_2 into the TiO_2 structure. The presence of a small amount of CeO_2 promoted the CO oxidation significantly, and the activities enhanced with the increase of CeO_2 amount, being Ir/$Ce_{0.2}$Ti the sample with the highest activity (Lu et al., 2023).

Ir-TiO_2 single-atom catalyst were prepared by Y Wang et al. The catalyst showed excellent low-temperature selective catalytic oxidation of ammonia. They found that rutile phase performed better than it counterpart anatase. Ir atoms had a better dispersion on rutile. The activity was related to the stronger electronic metal-support interaction with rutile than other phases 15 (Li et al., 2020).

C.B. Thompson studied the rate-controlled elementary steps for CO oxidation of the Ir-TiO_2 system. They showed that the supported Ir SACs were catalytically active for CO oxidation at atmospheric pressure and temperature ranges from 150°C to 200°C in 0.1%–10% CO and 1%–17% kPa O_2, providing insight into the reaction mechanism (Coogan et al., 2023).

Y. Lu studied SAC of Ir on $MgAl_2O_4$ for the CO oxidation reaction. They applied operando infrared and X-ray absorption spectroscopies and quantum chemical calculations to identify the Ir single-atom complex formed during CO oxidation. They found that Ir(CO) is the active complex, and the formation of Ir single-atom complex promotes the CO oxidation via an Eley–Rideal mechanism where Ir(CO) (O) is the resting state of the catalyst. Their results showed that strong adsorption by a ligand does not necessarily lead to catalyst poisoning due to the ability of single-atoms to bind to more than one ligand. DFT results indicated that Ir single atoms had a critical role in facilitating O_2 activation, while the CO ligand lowers the barrier for the Eley–Rideal rate-limiting step (Lu et al., 2019b).

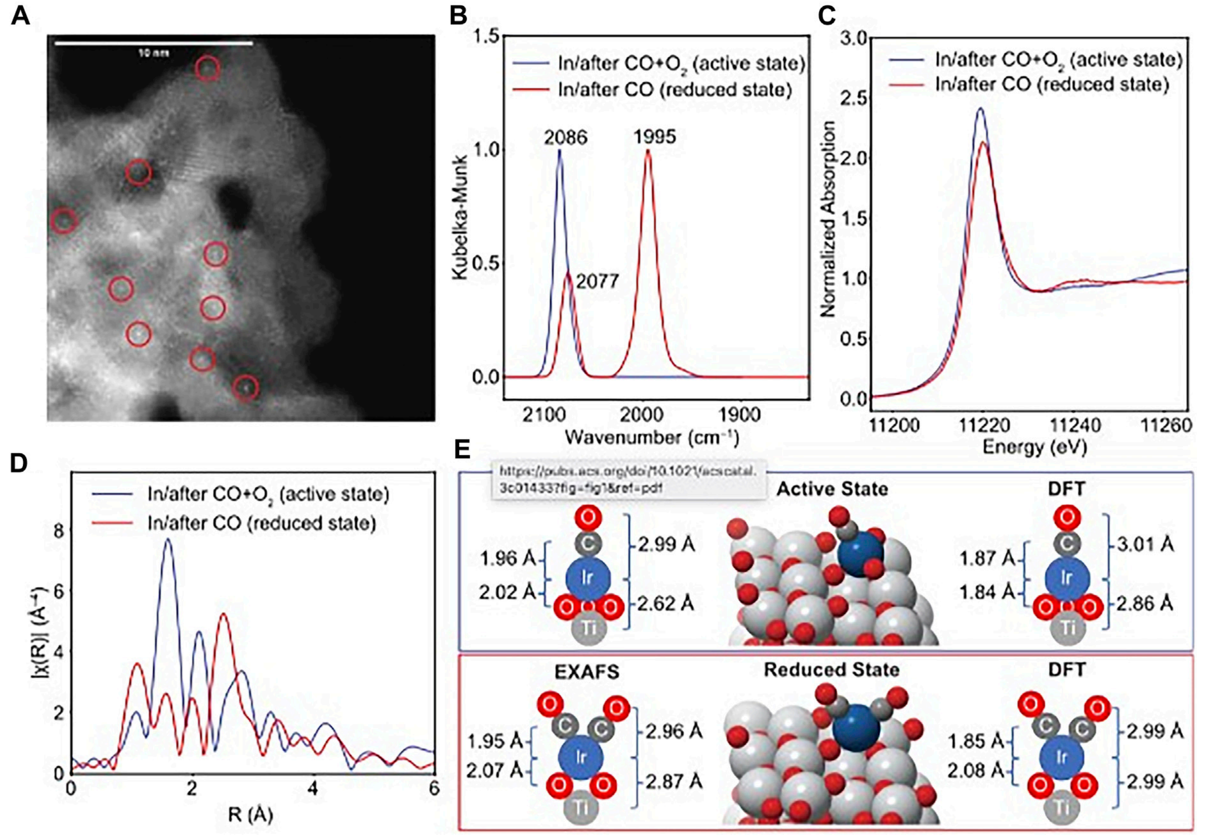

FIGURE 9
Ir/TiO_2 Characterization. **(A)** Scanning Transmission Electron Microscopy (STEM) image of the 0.1 wt% Ir/TiO_2 catalyst post-CO oxidation kinetic measurements at 170°C followed by CO reduction. **(B)** Differential Reflectance Infrared Fourier Transform (DRIFT) spectra recorded after CO oxidation at 170°C (blue) and post-reduction in CO at 170°C (red). **(C)** Ir-L_3 X-ray Absorption Near Edge Structure (XANES) spectra of the catalyst, showcasing the active state (blue) and the reduced state (red). **(D)** Magnitude component of the Fourier-transformed k3-weighted χ(k) data (Δk = 2.5–12 Å–1). For XANES/EXAFS, the reduced-state spectra were acquired in CO at 180°C, whereas the active-state spectra were recorded in CO and O_2 at 35°C, following CO oxidation at 195°C. **(E)** Representation of the local structures of Ir_1/TiO_2, combining experimental and theoretical insights. Color coding: O, red; Ti, silver; Ir, blue; C, gray. Reproduced from Coogan et al. (2023), with permission from Copyright © 2023 American Chemical Society.

5.2 Hydrogenation reactions

One of the first reports on single atom catalyst was done by Gates (Uzun et al., 2010). They reported the ethene hydrogenation by isolated atoms of Ir supported on MgO at room temperature and atmospheric pressure.

A dual single atom catalysts made of $IrMo/TiO_2$ was reported by J Fu and collaborators. The dual catalyst was consisted in discrete Ir single atoms and Mo single atoms anchored on TiO_2, showing great catalytic activity and chemoselectrivity in the hydrogenation of 4-nitrostyrene nad 4-vinylaniline that their monometallic counterparts. According to their density funcional theory calculations, they demonstrate that Ir sites were responsible for H_2 activation, while Mo sites were active site for the adsorption of 4-nitrostyrene via the nitro group (Fu et al., 2021).

A. Jia et al. (2023) reported the selective hydrogenation of crotonaldehyde (CROL) over Ir/TiO_2 catalyst. They studied the effect of metal size, from single atoms to nanoclusters (NC) to nanoparticles (NP), on the selective hydrogenation of this compound. Ir single atoms, clusters and nanoparticles were prepared on anatse TiO2. The reaction rates and TOFs of the different Ir/TiO_2 catalysts followed the order Ir(NP) > Ir(NC) > Ir(SA), while the selectivity was higher than 80% for Ir(SA) supported on TiO_2(101).

5.3 H_2 production

X Zhou and coworkers reported an approach to trap and stabilize Ir SACs on TiO_2 nanotubes, using the high density of Ti^{3+} - oxygen vacancies surface defect which served as highly effective SA iridium traps. The stably trapped SACs showed turnover frequencies of 4×10^6 h^{-1} in the photocatalytic H_2 production (Zhou et al., 2021).

5.4 Water gas shift

Ir_1/FeOx Single atom catalyst had a remarkable performance for water gas shift reaction, being superior to its Pt-based counterpart. Ir single atoms enhanced the reducibility of FeOx and generation of oxygen species (Luet al., 2019a).

5.5 Oxygen evolution reaction

MQ Yang et al. (2022) reported an strategy to improve the activity of Ir SACS by anchoring atomic Ir on oxygen vacancies of a $CoNiO_2$ support. The prepared SACs presented an overpotential of 183 mV at the current density was of 10 mA cm^{-2}, which was lower than a catalyst using Ir clusters.

The oxygen vacancies provided abundant active sites for the adsorption of OH* for OER. Based on Density Functional Theory (DFT) calculations, the enhanced activity of iridium (Ir) could be attributed to the Ir-S moiety in Ir_1/NFS, which is evident in the favorable formation of the *OOH intermediate during the Oxygen Evolution Reaction (OER) process (Lei et al., 2022).

L. Suhadolnik and collaborators prepared nanotubular TiOxNy-supported Ir single atoms, combined with clusters, as thin-film electrocatalysts. The nanomaterials consisted of a porous morphology. The catalyst exhibited very high oxygen evolution reaction activity in 0.1 M $HClO_4$, reaching 1,460 $Ag\text{-}_1Ir$ at 1.6 V *versus* a referente hydrogen electrode (Suhadolnik et al., 2023).

Yin et al. (2020) reported a strategy for the preparation of Ir single atoms supported on ultrathin $NiCo_2O_4$ porous nanosheets. The samples were produced by a co-elecgtrodeposition method. The catalysts showed higher OER activity and stability in acidic media due to the coupling of Ir single atoms with oxygen vacancies. An ultralow overpotencial of 240 mV a j = 10 $mAcm^{-2}$ was reported, with a long-term stabilty of 70 h. The surface electronic exchange-and-transfer activities of Ir atoms incorporated on the intrinsic oxygen vacancies of the metal support is the responsible to the high OER performance.

An influential work was done by Q. Wang and collaborators, who developed a catalyst consisted of a nickel oxide matrix, loaded with ultra-high content of Ir single atoms, up to 18 wt%. The catalyst showed enhanced OER in alkaline electrolyte, with an overpotential of 215 mV at 10 $mAcm^{-2}$, surprasing the activities of pure NiO and IrO2 catalyts. XPS and XANES results on the chemical state of Ir single atoms indicated that Ir was highly oxidized, with an oxidation state close to 4^+. After Ir doping, the oxidation state of Ni also modified, being higher than NiO. Ir atoms were well dispersed on the metal oxide surface with chemical bonding with the NiO substrate in a six-coordinated Ir – O (Wang et al., 2020).

5.6 Theoretical research

Undeniably, theoretical work on the interaction between metal atoms and molecules, as well as supports, have broaden the understanding of the behavior and stability of SACs. The calculations of their coordination environment and interactions have delivered important information on the single atom's contribution to the catalytic activity for different reactions.

For instance, Lin et al. (2020) studied the molecular adsorption properties of CH_4 on single atoms supported on anatase TiO_2(101) using the first-principles method based on density functional theory (DFT). The calculated formation energy of Ir-TiO_2 was de lowest, compare to other noble metal systems. Their results showed that Ir was the most stable system.

In their theoretical work, V. Fung and collaborators reported that single atoms dispersed on TiO_2 acomplish strong methane chemisorption and facle C-H activations. The calculations for chemisorption of methane were done by replacing a surface Ti atom (110) with the single metallic atom, coordinated to four surface oxygens and one subsurface oxygen. The coordination to the rutile TiO_2 surface modified the electronic structure of the single atoms site for chemisorption. They showed that Ir single atoms and other SACs on rutile TiO_2(119) can active C-H of methane at low temperature. Methane adsorption was found to be stronger on the single atom site on the rutile (110) surface than on the anatase (101) surface, with Ir and Pt single atoms being the metals with stronger CH_4 adsorption (Fung et al., 2018).

6 Future challenges

Several challenges exist for the practical implementation of Ir SACs, with a primary concern being the enhancement of the metal-support interaction. Potential strategies include investigating the DPU synthesis method, employing the impregnation method, and exploring in situ-synthesis techniques with low metal loading. Furthermore, a comprehensive characterization of the Ir-$TiO_{2\text{-rutile}}$ surface through XAS, XPS, HR-STEM, and DRIFT studies is essential to improve the catalyst's performance. Additionally, an evaluation of its activity, such as CO conversion, for comparative analysis with existing Ir/TiO_2 systems is crucial. Finally, the application of DFT studies to examine Iridium-SACs in various facets of TiO_2 may yield valuable insights into their catalytic behavior. It is imperative to continue studying the mechanisms involved during the catalytic processes to gain a better understanding of the contributions of Ir SACs. There are still few reports on this area and further research is of great importance.

7 Conclusion

In conclusion, despite the challenges involved in the synthesis and characterization of single atom catalysts (SACs), this study demonstrates the successful deposition of iridium as isolated atoms on TiO_2. The presence of these iridium atoms on the catalyst surface has been confirmed, highlighting the potential of TiO_2 as a suitable support for SACs. Furthermore, the reactivity of these isolated iridium atoms in catalytic reactions has been observed, emphasizing their functional role in driving catalytic processes.

The ability to deposit and retain iridium atoms as isolated entities on the TiO_2 support opens up new possibilities for the design and development of highly efficient catalysts. The presence of these reactive iridium species on the catalyst surface offers enhanced catalytic performance and selectivity. Despite the challenges associated with the synthesis and characterization of SACs, the findings from this study demonstrate the feasibility of achieving and maintaining isolated iridium atoms on the TiO_2 support, providing valuable insights for future catalyst design and optimization.

Overall, the successful deposition of isolated iridium atoms on TiO_2, their retention on the support surface, and their reactivity in catalysis highlight the promising potential of SACs in various catalytic applications. Further research and development efforts are warranted to fully explore and harness the capabilities of SACs supported on TiO_2, with the aim of advancing catalytic technologies and addressing current environmental and energy challenges.

Author contributions

MM-T: Conceptualization, Investigation, Writing–original draft. OH-C: Supervision, Validation, Writing–review and editing. RM-C: Conceptualization, Funding acquisition, Supervision, Validation, Writing–review and editing.

Funding

The authors declare financial support was received for the research, authorship, and/or publication of this article. The research was founded by Dirección General de Asuntos del Personal Académico (DGAPA) through grant PAPIIT IA-106623.

Acknowledgments

Acknowledgments to Dr. Gabriela Díaz-Guerrero, Dr. Rodolfo Zanella Specia, Dr. Raúl Herrera, Dr. Antonio Gómez-Cortés, Phys. Josué Romero, Dr. Lourdes Bazán, Dr. Omar Novelo, M.S Ana Karla Bobadilla, Phys. Lázaro Huerta Arcos, M.S. Adriana Tejeda, M.S. Viridiana Maturano Rojas, M.S. Alejandro Pompa-García, Dr. Samuel Tehuacanero-Cuapa, and Eng. Cristina Zorrilla for all the scientific and technical support provided.

Conflict of interest

Publisher's note

References

Bhirud, V. A., Uzun, A., Kletnieks, P. W., Craciun, R., Haw, J. F., Dixon, D. A., et al. (2007). Synthesis and crystal structure of Ir(C2H4)2(C5H7O2). *J. Organomet. Chem.* 692 (10), 2107–2113. doi:10.1016/j.jorganchem.2007.01.008

Bokhimi, X., Zanella, R., Morales, A., Maturano, V., and Ángeles-Chávez, C. (2011). Au/rutile catalysts: effect of the activation atmosphere on the gold-support interaction. *J. Phys. Chem. C* 115 (13), 5856–5862. doi:10.1021/jp111483v

Cao, W., Lu, L., Qi, H., Qian, He, Wu, Z., Wang, A., et al. (2019), *In-situ* synthesis of single-atom Ir by utilizing metal-organic frameworks: an acid-resistant catalyst for hydrogenation of levulinic acid to γ-valerolactone. *J. Catal.* 373, 161–172. doi:10.1016/j.jcat.2019.03.035

Carter, C. B., and Williams, D. B. (2016). *Transmission electron microscopy: Diffraction, imaging, and spectrometry*. Berlin, Germany: Springer.

Carter, D. B. W. C. B. (2009). *Transmission electron microscopy A textbook for materials science.* Berlin, Germany: Springer publication.

Cescor, (2023). Cescor - Cs-corrector for stem. https://www.ceos-gmbh.de/en/produkte/stemkorrektoren/cescor.

Chen, Y., Ji, S., Chen, C., Peng, Q., Wang, D., and Li, Y. (2018). Single-atom catalysts: synthetic strategies and electrochemical applications. *Joule* 2 (7), 1242–1264. doi:10.1016/j.joule.2018.06.019

Coogan, B., Liping, L., Leshchev, D. S., Hoffman, A. S., Hong, J., Bare, S. R., et al. (2023). CO oxidation on Ir1/TiO2: resolving ligand dynamics and elementary reaction steps. *ACS Catal.* 13 (12), 7802–7811. doi:10.1021/acscatal.3c01433

Cui, T., Li, L., Ye, C., Li, X., Liu, C., Zhu, S., et al. (2022). Heterogeneous single atom environmental catalysis: fundamentals, applications, and opportunities. *Adv. Funct. Mater.* 32 (9), 2108381. doi:10.1002/adfm.202108381

de Vries, J., and Jackson, S. (2012). Homogeneous and heterogeneous catalysis in industry. *Catal. Sci. Technol.* 2, 2009. doi:10.1039/C2CY90039D

Deepak, F. L., Mayoral, A., and Arenal, R. (2015). *Advanced transmission electron microscopy: Applications to nanomaterials.* Berlin, Germany: Springer.

Díaz, G., Gómez-Cortés, A., Hernández-Cristobal, O., Murcia, J. J., Borda, G., and Rojas, H. (2011). Hydrogenation of citral over IrAu/TiO2 catalysts. Effect of the preparation method. *Top. Catal.* 54, 467–473. doi:10.1007/s11244-011-9609-x

Erdoğan, H., Metin, Ö., and Özkar, S. (2009). *In situ*-generated PVP-stabilized palladium(0) nanocluster catalyst in hydrogen generation from the methanolysis of ammonia–borane. *Phys. Chem. Chem. Phys.* 11 (44), 10519. doi:10.1039/b916459f

Fu, J., Dong, J., Si, R., Sun, K., Zhang, J., Li, M., et al. (2021). Synergistic effects for enhanced catalysis in a dual single-atom catalyst. *ACS Catal.* 11 (4), 1952–1961. doi:10.1021/acscatal.0c05599

Fung, V., Tao, F., Feng), and Jiang, D. (2018). Low-temperature activation of methane on doped single atoms: descriptor and prediction. *Phys. Chem. Chem. Phys.* 20 (35), 22909–22914. doi:10.1039/C8CP03191F

Gómez-Cortés, A., Díaz, G., Zanella, R., Ramírez, H., Santiago, P., and JoséSaniger, M. (2009). Au–Ir/TiO$_2$ prepared by deposition precipitation with urea: improved activity and stability in CO oxidation. *J. Phys. Chem. C* 113 (22), 9710–9720. doi:10.1021/jp810905n

Greczynski, G., and Hultman, L. (2020). X-Ray photoelectron spectroscopy: towards reliable binding energy referencing. *Prog. Mater. Sci.* 107, 100591. doi:10.1016/j.pmatsci.2019.100591

Guo, J., Liu, H., Li, D., Wang, J., Djitcheu, X., He, D., et al. (2022). A minireview on the synthesis of single atom catalysts. *RSC Adv.* 12 (15), 9373–9394. doi:10.1039/D2RA00657J

Haruta, M., Kobayashi, T., Sano, H., and Yamada, N. (1987). Novel gold catalysts for the oxidation of carbon monoxide at a temperature far below 0 C. *Chem. Lett.* 16 (2), 405–408. doi:10.1246/cl.1987.405

Haruta, M. (1997). Novel catalysis of gold deposited on metal oxides. *Catal. Surv. Asia* 1 (1), 61–73. doi:10.1023/A:1019068728295

Herzing, A. A., Kiely, C. J., Carley, A. F., Landon, P., and Hutchings, G. J. (2008). Identification of active gold nanoclusters on iron oxide supports for CO oxidation. *Science* 321 (5894), 1331–1335. doi:10.1126/science.1159639

Jia, A., Zhang, W., Peng, H., Zhang, Y., Song, T., Li, L., et al. (2023). Selective hydrogenation of crotonaldehyde over Ir/TiO2 catalysts: unraveling the metal-support interface related reaction mechanism. *J. Catal.* 425, 57–69. doi:10.1016/j.jcat.2023.05.029

Kim, A., Debecker, D. P., Devred, F., Dubois, V., Sanchez, C., and Sassoye, C. (2018). CO2 methanation on Ru/TiO2 catalysts: on the effect of mixing anatase and rutile TiO2 supports. *Appl. Catal. B Environ.* 220, 615–625. doi:10.1016/j.apcatb.2017.08.058

Kominami, H., Kato, J. I., Takada, Y., Doushi, Y., Ohtani, B., Nishimoto, S. I., et al. (1997). Novel synthesis of microcrystalline titanium (IV) oxide having high thermal stability and ultra-high photocatalytic activity: thermal decomposition of titanium (IV) alkoxide in organic solvents. *Catal. Lett.* 46 (3-4), 235–240. doi:10.1023/A:1019022719479

Koningsberger, D. C., and Prins, (1987). *R. X-ray absorption: Principles, applications, techniques of EXAFS, SEXAFS and XANES.* Hoboken, New Jersey, United States: Wiley.

Kottwitz, M., Li, Y., Wang, H., Frenkel, A. I., and Nuzzo, R. G. (2021). Single atom catalysts: A review of characterization methods. *Chem. - Methods* 1, 278–294. doi:10.1002/cmtd.202100020

Lebedev, D., Ezhov, R., Heras-Domingo, J., Comas-Vives, A., Kaeffer, N., Willinger, M., et al. (2020). Atomically dispersed iridium on indium tin oxide efficiently catalyzes water oxidation. *ACS Central Sci.* 6 (7), 1189–1198. doi:10.1021/acscentsci.0c00604

Lee, M., Arras, R., Takahashi, R., Warot-Fonrose, B., Daimon, H., Marie-José, C., et al. (2018). Noble metal nanocluster formation in epitaxial perovskite thin films. *ACS Omega* 3 (2), 2169–2173. doi:10.1021/acsomega.7b02071

Lei, Z., Cai, W., Rao, Y., Wang, K., Jiang, Y., Liu, Y., et al. (2022). Coordination modulation of iridium single-atom catalyst maximizing water oxidation activity. *Nat. Commun.* 13, 24. doi:10.1038/s41467-021-27664-z

Li, Z., Chen, Y., Ji, S., Tang, Y., Chen, W., Li, A., et al. (2020). Iridium single-atom catalyst on nitrogen-doped carbon for formic acid oxidation synthesized using a general host–guest strategy. *Nat. Chem.* 12, 764–772. doi:10.1038/s41557-020-0473-9

Li, Z., Ji, S., Liu, Y., Cao, X., Tian, S., Chen, Y., et al. (2019). Well-defined materials for heterogeneous catalysis: from nanoparticles to isolated single-atom sites. *Chem. Rev.* 120, 623–682. doi:10.1021/acs.chemrev.9b00311

Liang, H., Chen, G., Desinan, S., Rosei, R., Rosei, F., and Ma, D. (2012). *In situ* facile synthesis of ruthenium nanocluster catalyst supported on carbon black for hydrogen generation from the hydrolysis of ammonia-borane. *Int. J. Hydrogen Energy* 37 (23), 17921–17927. doi:10.1016/j.ijhydene.2012.09.026

Lin, J., Wang, A., Qiao, B., Liu, X., Yang, X., Wang, X., et al. (2013). Remarkable performance of Ir_1/FeO_x single-atom catalyst in water gas shift reaction. *J. Am. Chem. Soc.* 135 (41), 15314–15317. doi:10.1021/ja408574m

Lin, J., Qiao, B., Liu, J., Huang, Y., Wang, A., Li, L., et al. (2012). Design of a highly active $Ir/Fe(OH)_x$Catalyst: versatile application of Pt-group metals for the preferential oxidation of carbon monoxide. *Angew. Chem. Int. Ed.* 51 (12), 2920–2924. doi:10.1002/anie.201106702

Lin, L., Shi, Z., Huang, J., Wang, P., Yu, W., He, C., et al. (2020). Molecular adsorption properties of CH4 with noble metals doped onto oxygen vacancy defect of anatase TiO2 (101) surface: first-principles calculations. *Appl. Surf. Sci.* 514, 145900. doi:10.1016/j.apsusc.2020.145900

Lu, D., Li, B., Peng, Y., Hao, X., Xuan, R., Huang, H., et al. (2023). Tuning interaction strength between CeO2 and iridium to promote CO oxidation over Ir/TiO2. *J. Rare Earths*, 1002–0721. doi:10.1016/j.jre.2023.05.006

Lu, Y., Kuo, C.-Te, Kovarik, L., Hoffman, A. S., Boubnov, A., Driscoll, D. M., et al. (2019a). A versatile approach for quantification of surface site fractions using reaction kinetics: the case of CO oxidation on supported Ir single atoms and nanoparticles. *J. Catal.* 378, 121–130. doi:10.1016/j.jcat.2019.08.023

Lu, Y., Wang, J., Yu, L., Kovarik, L., Zhang, X., Hoffman, A. S., et al. (2019b). Identification of the active complex for CO oxidation over single-atom Ir-on-$MgAl_2O_4$ catalysts. *Nat. Catal.* 2, 149–156. doi:10.1038/s41929-018-0192-4

Milone, C., Trapani, M., Zanella, R., Piperopolulos, E., and Galvagno, S. (2010). Deposition-precipitation with urea to prepare Au/Mg(OH)2 catalysts: influence of the preparation conditions on metal size and load. *Mater. Res. Bull.* 45 (12), 1925–1933. doi:10.1016/j.materresbull.2010.08.014

Mitchell, M. B. (1993). *Fundamentals and applications of diffuse reflectance infrared fourier transform (DRIFT) spectroscopy*. Washington, D.C. USA: ACS Publications, 351–375. doi:10.1021/ba-1993-0236.ch013

Monteseguro, V., Sans, J. A., Cuartero, V., Cova, F., Abrikosov, I. A., Olovsson, W., et al. (2020). Single-atom catalysts across the periodic table. *Chem. Rev.* 120, 11703–11809. doi:10.1021/acs.chemrev.0c00576

Norman, D. (1986). X-ray absorption spectroscopy (EXAFS and XANES) at surfaces. *J. Phys. C Solid State Phys.* 19 (18), 3273–3311. doi:10.1088/0022-3719/19/18/006

Oswald, S. (2013). "X-ray photoelectron spectroscopy in analysis of surfaces update based on the original article by steffen oswald, encyclopedia of analytical chemistry," in *Encyclopedia of analytical chemistry*. Editors R. A. Meyers and R. A. Meyers (Hoboken, New Jersey, United States: John Wiley & Sons, Ltd). doi:10.1002/9780470027318.a2517.pub2

Palcheva, R., Dimitrov, L., Tyuliev, G., Spojakina, A., and Jiratova, K. (2013). TiO2 nanotubes supported NiW hydrodesulphurization catalysts: characterization and activity. *Appl. Surf. Sci.* 265, 309–316. doi:10.1016/j.apsusc.2012.11.001

Pascarelli, S., Garbarino, G., Jönsson, H. J. M., Irifune, T., Errandonea, D., Olovsson, W., et al. (2019). Phase stability and electronic structure of iridium metal at the megabar range. *Sci. Rep.* 9 (1), 8940. doi:10.1038/s41598-019-45401-x

Pawluk, T., Hirata, Y., and Wang, L. (2005). Studies of iridium nanoparticles using density functional theory calculations. *J. Phys. Chem. B* 109 (44), 20817–20823. doi:10.1021/jp053563b

Pennycook, S. J., and Nellist, P. D. (2011). *Scanning transmission electron microscopy: Imaging and analysis*. Berlin, Germany: Springer Science & Business Media.

Pham, H. Q., Pham, H. T. Q., Huynh, Q., and Huynh, T. T. (2023). Single-atom iridium-based catalysts: synthesis strategies and electro(photo)-catalytic applications for renewable energy conversion and storage. *Coord. Chem. Rev.* 486, 215143. doi:10.1016/j.ccr.2023.215143

Plascencia-Villa, G., Mendoza-Cruz, R., Bazán-Díaz, L., and José-Yacamán, M. (2020). Gold nanoclusters, gold nanoparticles, and analytical techniques for their characterization. *Nanoparticles Biol. Med. Methods Protoc.* 2118, 351–382. doi:10.1007/978-1-0716-0319-2_26

Plascencia-Villa, G., and Mendoza-Cruz, R. (2022). "Gold nanoparticles for biocatalysis," in *Nanomaterials for biocatalysis* (Amsterdam, Netherlands: Elsevier), 377–434.

Qiao, B., Wang, A., Yang, X., Allard, L. F., Jiang, Z., Cui, Y., et al. (2011). Single-atom catalysis of CO oxidation using Pt1/FeOx. *Nat. Chem.* 3, 634–641. doi:10.1038/nchem.1095

Qin, H., Tan, X., Huang, W., Jiang, J., and Jiang, H. (2015). Application of urea precipitation method in preparation of advanced ceramic powders. *Ceram. Int.* 41 (9), 11598–11604. doi:10.1016/j.ceramint.2015.06.032

Ramaker, D. E., and Koningsberger, D. C. (2010). The atomic AXAFS and Δμ XANES techniques as applied to heterogeneous catalysis and electrocatalysis. *Phys. Chem. Chem. Phys.* 12 (21), 5514. doi:10.1039/b927120c

Ramos-Delgado, N. A., Gracia-Pinilla, M. Á., Mangalaraja, R. V., O'Shea, K., and Dionysiou, D. D. (2016). Industrial synthesis and characterization of nanophotocatalysts materials: titania. *Nanotechnol. Rev.* 5 (5), 467–479. doi:10.1515/ntrev-2016-0007

Remediakis, I. N., Lopez, N., and Nørskov, J. K. (2005). CO oxidation on rutile-supported Au nanoparticles. *Angew. Chem. Int. Ed.* 44, 1824–1826. doi:10.1002/anie.200461699

Rojas, H. A., Martínez, J. J., Díaz, G., and Gómez-Cortés, A. (2015). The effect of metal composition on the performance of Ir–Au/TiO2 catalysts for citral hydrogenation. *Appl. Catal. A General* 503, 196–202. doi:10.1016/j.apcata.2015.07.023

Samantaray, M. K., D'Elia, V., Pump, E., Falivene, L., Harb, M., Ould Chikh, S., et al. (2020). The comparison between single atom catalysis and surface organometallic catalysis. *Chem. Rev.* 120 (2), 734–813. doi:10.1021/acs.chemrev.9b00238

Sayers, D. E., Lytle, F. W., and Stern, E. A. (1970). *Advances in X-ray analysis*. New York, NY, USA: Plenum.

Sayers, D. E., Stern, E. A., and Lytle, F. W. (1971). New technique for investigating noncrystalline structures: fourier analysis of the extended X-ray—absorption fine structure. *Phys. Rev. Lett.* 27 (18), 1204–1207. doi:10.1103/physrevlett.27.1204

Scirè, S., Fiorenza, R., Bellardita, M., and Palmisano, L. (2021). "Catalytic applications of TiO2," in *Titanium dioxide (TiO) and its applications* (Amsterdam, Netherlands: Elsevier), 637–679. doi:10.1016/B978-0-12-819960-2.00006-7

Shan, J., Ye, C., Jiang, Y., Jaroniec, M., Zheng, Y., and Qiao, S. Z. (2022). Metal-metal interactions in correlated single-atom catalysts. *Sci. Adv.* 8 (17), eabo0762. doi:10.1126/sciadv.abo0762

Shan, J., Ye, C., Chen, S., Sun, T., Jiao, Y., Liu, L., et al. (2021). Short-range ordered iridium single atoms integrated into cobalt oxide spinel structure for highly efficient electrocatalytic water oxidation. *J. Am. Chem. Soc.* 143 (13), 5201–5211. doi:10.1021/jacs.1c01525

Shao, X., Yang, X., Xu, J., Liu, S., Miao, S., Liu, X., et al. (2019a). Iridium single-atom catalyst performing a quasi-homogeneous hydrogenation transformation of CO2 to formate. *Chem* 5, 693–705. doi:10.1016/j.chempr.2018.12.014

Shao, X., Yang, X., Xu, J., Liu, S., Miao, S., Liu, X., et al. (2019b). Iridium single-atom catalyst performing a quasi-homogeneous hydrogenation transformation of CO2 to formate. *Chem* 5, 693–705. doi:10.1016/j.chempr.2018.12.014

Suhadolnik, L., Bele, M., Čekada, M., Jovanovič, P., Maselj, N., Lončar, A., et al. (2023). Nanotubular TiO_xN_y-supported Ir single atoms and clusters as thin-film electrocatalysts for oxygen evolution in acid media. *Chem. Mater.* 35 (6), 2612–2623. doi:10.1021/acs.chemmater.3c00125

Sun, L., Liang, X., Liu, H., Cao, H., Liu, X., Jin, Y., et al. (2023). Activation of Co-O bond in (110) facet exposed Co3O4 by Cu doping for the boost of propane catalytic oxidation. *J. Hazard. Mater.* 452, 131319. doi:10.1016/j.jhazmat.2023.131319

Tauster, S. J., Fung, S. C., Baker, R. T. K., and Horsley, J. A. (1981). Strong interactions in supported-metal catalysts. *Science* 211 (4487), 1121–1125. doi:10.1126/science.211.4487.1121

Turner, M., Golovko, V., Vaughan, O., Abdulkin, P., Berenguer-Murcia, A., Tikhov, M., et al. (2008). Selective oxidation with dioxygen by gold nanoparticle catalysts derived from 55-atom clusters. *Nature* 454, 981–983. doi:10.1038/nature07194

Uzun, A., Ortalan, V., Browing, N. D., and Gates, B. C. (2010). A site-isolated mononuclear iridium complex catalyst supported on MgO: characterization by spectroscopy and aberration-corrected scanning transmission electron microscopy. *J. Catal.* 269 (2), 318–328. doi:10.1016/j.jcat.2009.11.017

Vaithianathan, V., Lee, B.-T., Chang, C.-H., Asokan, K., and Kim, S. S. (2006). Characterization of As-doped, p-type ZnO by x-ray absorption near-edge structure spectroscopy. *Appl. Phys. Lett.* 88 (11), 112103. doi:10.1063/1.2186383

Van Dillen, A. J., Terörde, R. J. A. M., Lensveld, D. J., Geus, J. W., and de Jong, K. P. (2003). Synthesis of supported catalysts by impregnation and drying using aqueous chelated metal complexes. *J. Catal.* 216 (1–2), 257–264. doi:10.1016/S0021-9517(02)00130-6

Wang, Q., Huang, X., Zhao, Z. L., Wang, M., Xiang, B., Li, J., et al. (2020). Ultrahigh-loading of Ir single atoms on NiO matrix to dramatically enhance oxygen evolution reaction. *J. Am. Chem. Soc.* 142, 7425–7433. doi:10.1021/jacs.9b12642

Wang, Y., Xu, W., Chen, X., Li, C., Xie, J., Yang, Y., et al. (2022). Single–atom Ir1 supported on rutile TiO2 for excellent selective catalytic oxidation of ammonia. *J. Hazard. Mater.* 432 (128670), 128670. doi:10.1016/j.jhazmat.2022.128670

Xia, C., Qiu, Y., Xia, Y., Zhu, P., King, G., Zhang, X., et al. (2021). General synthesis of single-atom catalysts with high metal loading using graphene quantum dots. *Nat. Chem.* 13, 887–894. doi:10.1038/s41557-021-00734-x

Xiao, M., Zhu, J., Li, G., Li, N., Li, S., Cano, Z. P., et al. (2019). A single-atom iridium heterogeneous catalyst in oxygen reduction reaction. *Angew. Chem. Int. Ed.* 58, 9640–9645. doi:10.1002/anie.201905241

Xiong, Y., Sun, W., Xin, P., Chen, W., Zheng, X., Yan, W., et al. (2020). Gram-scale synthesis of high-loading single-atomic-site fe catalysts for effective epoxidation of styrene. *Adv. Mater.* 32, 2000896. doi:10.1002/adma.202000896

Yang, H., Wang, X., Liu, Q., Huang, A., Zhang, X., Yi, Yu, et al. (2023). Heterogeneous iridium single-atom molecular-like catalysis for epoxidation of ethylene. *J. Am. Chem. Soc.* 145 (12), 6658–6670. doi:10.1021/jacs.2c11380

Yang, M.-Q., Zhou, K.-L., Wang, C., Zhang, M.-C., Wang, C.-H., Ke, X., et al. (2022). Iridium single-atom catalyst coupled with lattice oxygen activated CoNiO2 for accelerating the oxygen evolution reaction. *J. Mater. Chem. A* 10 (48), 25692–25700. doi:10.1039/D2TA07292K

Yang, X.-F., Wang, A., Qiao, B., Li, J., Liu, J., and Zhang, T. (2013). Single-atom catalysts: A new frontier in heterogeneous catalysis. *Accounts Chem. Res.* 46 (8), 1740–1748. doi:10.1021/ar300361m

Yin, J., Jin, J., Lu, M., Huang, B., Zhang, H., Peng, Y., et al. (2020). Iridium single atoms coupling with oxygen vacancies boosts oxygen evolution reaction in acid media. *J. Am. Chem. Soc.* 142 (43), 18378–18386. doi:10.1021/jacs.0c05050

Zanella, R., Delannoy, L., and Louis, C. (2005). Mechanism of deposition of gold precursors onto TiO2 during the preparation by cation adsorption and deposition-precipitation with NaOH and urea. *Appl. Catal. A General* 291 (1–2), 62–72. doi:10.1016/j.apcata.2005.02.045

Zhang, M., Sui, X., Zhang, X., Niu, M., Li, C., Wan, H., et al. (2022). Multi-defects engineering of NiCo2O4 for catalytic propane oxidation. *Appl. Surf. Sci.* 600, 154040. doi:10.1016/j.apsusc.2022.154040

Zhang, N., Wang, W., Zhou, T., Tian, Y., and Chu, W. (2021). Exploring structure-function relationship of two-dimensional electrocatalysts with synchrotron radiation X-ray absorption spectrum. *Curr. Chin. Sci.* 1 (1), 22–42. doi:10.2174/2210298101999201008142619

Zhao, J., Ji, S., Guo, C., Li, H., Dong, J., Guo, P., et al. (2021). A heterogeneous iridium single-atom-site catalyst for highly regioselective carbenoid O–H bond insertion. *Nat. Catal.* 4, 523–531. doi:10.1038/s41929-021-00637-7

Zhou, X., Hwang, I., Tomanec, O., Fehn, D., Mazare, A., Zboril, R., et al. (2021). Advanced photocatalysts: pinning single atom co-catalysts on titania nanotubes. *Adv. Funct. Mater.* 31 (30), 2102843. doi:10.1002/adfm.202102843

Zhu, Y., Wang, J., Koketsu, T., Kroschel, M., Chen, J. M., Hsu, S. Y., et al. (2022b). Iridium single atoms incorporated in Co3O4 efficiently catalyze the oxygen evolution in acidic conditions. *Nat. Commun.* 13, 7754. doi:10.1038/s41467-022-35426-8

Zhu, Y., Wang, J., Koketsu, T., Kroschel, M., Chen, J. M., Hsu, S. Y., et al. (2022a). Iridium single atoms incorporated in Co3O4 efficiently catalyze the oxygen evolution in acidic conditions. *Nat. Commun.* 13 (1), 7754. doi:10.1038/s41467-022-35426-8

Zonghua, pu, Ibrahim, A., Cheng, R., Wang, P., Zhang, C., Mu, S., et al. (2020). Single-atom catalysts for electrochemical hydrogen evolution reaction: recent advances and future perspectives. *Nano-Micro Lett.* 12, 21. doi:10.1007/s40820-019-0349-y